

Electro-click construction of Hybrid Nanocapsule Films with Triggered Delivery Properties

Flavien Sciortino^{†a*}, Gauthier Rydzek^{†b*}, Fabien Grasset^c, Myrtil L. Kahn^d, Jonathan P. Hill^b, Soizic Chevance^a, Fabienne Gauffre^a, Katsuhiko Ariga^{b,e}

† These authors contributed equally

^a Institut des Sciences Chimiques de Rennes, UMR 6226, CNRS, Université de Rennes 1, 263 av. General Leclerc, 35042 Rennes Cedex, France

^b World Premier International (WPI) Research Center for Materials Nanoarchitectonics (MANA), National Institute for Materials Science (NIMS), 1-1 Namiki, Tsukuba 305-0044, Japan

^c UMI 3629 CNRS - Saint Gobain – NIMS, Laboratory for Innovative Key Materials and Structures (LINK), National Institute for Materials Science (NIMS), 1-1 Namiki, Tsukuba 305-0044, Japan

^d Laboratoire de Chimie de Coordination UPR8241 CNRS, 205 rte de Narbonne, 31000 Toulouse Cedex 04, France.

^e Graduate School of Frontier Science, The University of Tokyo, Kashiwa 277-0827, Japan

Corresponding Authors: RYDZEK.Gauthier@nims.go.jp, flavien.sciortino@univ-rennes1.fr

Supporting Information

Figure S-1: Size characterization of the inorganic nanoparticles and of hybridosomes.

Video S-1: TEM tomography of a single Hybridosome®.

Scheme S-1: Grafting degree of PAA-C≡CH.

Scheme S-2: Grafting degree of PEI-C≡C.

Figure S-2: ATR-FTIR Spectroscopy of functionalized polymers.

Figure S-3: Buildup of the film.

Figure S-4: Click reaction occurrence.

Figure S-5: Evolution of the intensity-potential diagram during the film construction.

Table S-1: Evolution of the film roughnesses during the electroclick deposition process.

Figure S-6: Film growth, thickness evolution.

Figure S-7: Chemical and structural stability of Hybridosomes® along the process of film construction.

Figure S-8: Chemical composition of films constructed with IONPs based Hybridosomes®.

Figure S-9: Bodipy encapsulation, UV/Vis and Fluorescence spectra.

Figure S-10: Loading efficiency of Hybridosomes.

Figure S-11: Surface area of fluorescence emission bands.

Figure S-12: pH sensitivity of functional clickable Hybridosome® dispersions.

Figure S-13: pH sensitivity of electro-clicked Hybridosome®-based films.

Figure S-14: pH-triggered release abilities of electro-clicked Hybridosomes®-based films.

Figure S-15: Cargo release under electrochemical stimulus.

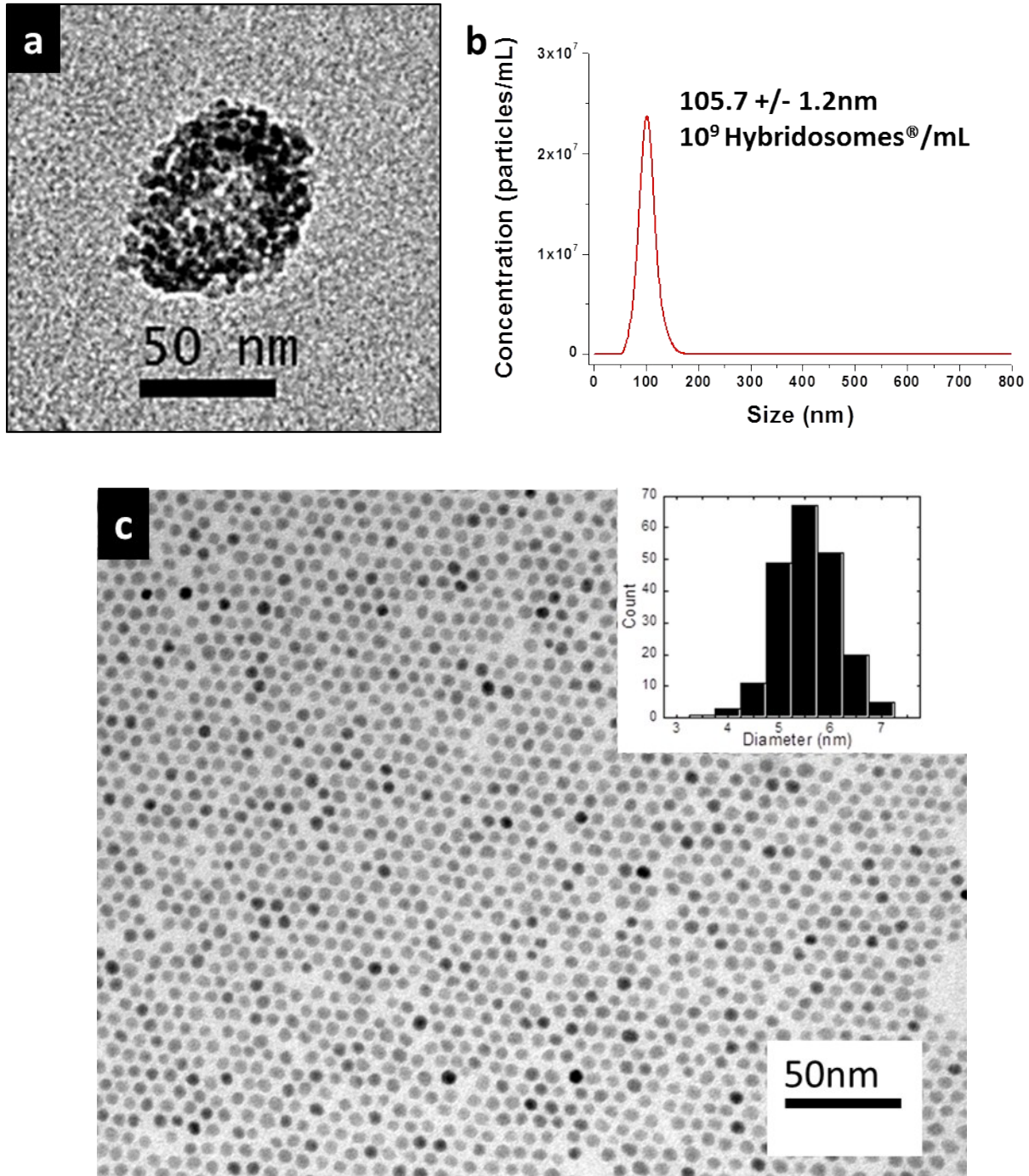


Figure S-1: Size characterization of the inorganic nanoparticles and of hybridosomes. a) TEM micrograph of a single Hybridosome corresponding to the first slice of the S-1 video. b) Size distribution of a Hybridosome in aqueous dispersion, measured by Nanoparticles Tracker Analysis (NTA), which allows the mean-size and the concentration of Hybridosomes suspensions to be calculated. NTA tracks individual trajectories, allowing the calculation of the diffusion coefficient and thus of the hydrodynamic diameter of each particle. NTA was carried out with a Nanosight LM10 device system equipped with a 40 mW laser working at $\lambda = 638$ nm. Video sequences were recorded via a CCD camera operating at 30 frames per second and evaluated via the NANOSIGHT NTA 2.0 Analytical Software Suite. The hybridosomes suspensions at $[\text{Fe}] \sim 50 \mu\text{g/mL}$ are washed two times after magnetic separation and diluted 100 times before NTA analysis. c) Characteristic TEM picture and size histogram distribution of pristine iron oxide nanoparticles.

Video S-1: TEM tomography of a single Hybridosome®.

Reconstructed video obtained from 76 tomography-slices measured from -60° to $+15^\circ$ with a 1° increment.

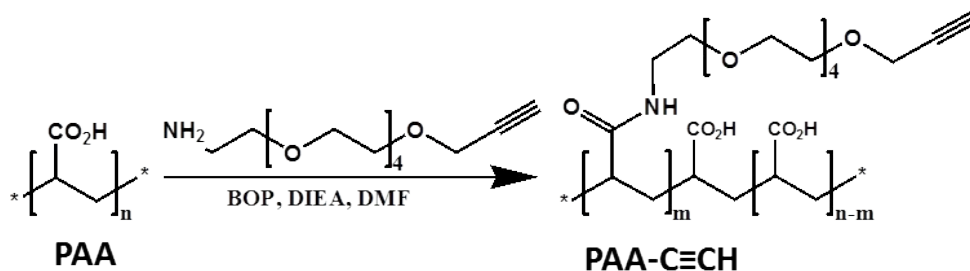
<https://mycore.core-cloud.net/public.php?service=files&t=10205a71e3d5fd4d80dc4370f2b0812c>

Polymer grafting degrees.

- Estimation of the grafting degree of PAA-C≡CH by ^1H NMR.

We arbitrarily fixed the integration value of the alkyne CCH signal of PEG (2.83 ppm) at 1. From a comparison of the integration values of signals between 3.72-3.16 ppm (NHCH₂, CH₂NH, CH₂OCH₂ of PEG) and those between 2.52 -1.37 ppm (CH₂CHCO of PAA and CH₂CH₂CH₂CCH of PEG), the effective degree of modification was estimated to be 6%.

^1H NMR assignment in ppm (500 MHz, 10% D₂O): 8,07 (b, CONHCH₂), 4,16 (s, OCH₂CCH), 3,67 (bm, CONHCH₂CH₂O), 3,62 (bs, OCH₂CH₂O), 3,52 (bm, CONHCH₂CH₂O), 2,83 (s, OCH₂CH₂CCH), 2,29 (b, CH(COOH)CH₂), 1,82 (b, CHCH₂), 1,64 (b, CH(COOH)CH₂), 1,53 (b, CH₃CH).

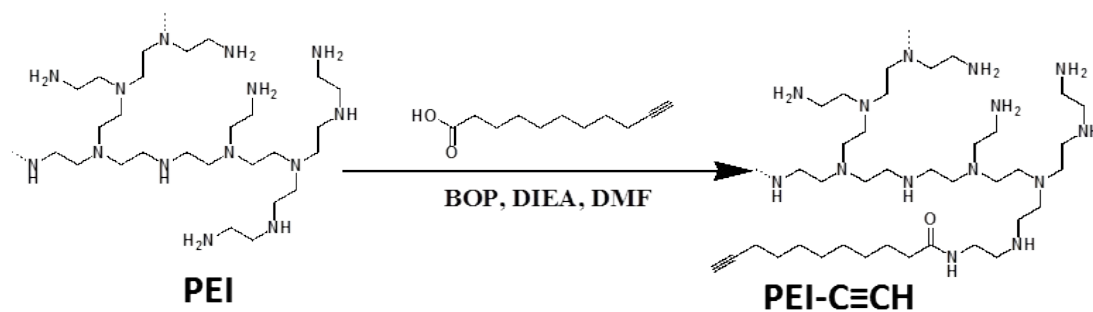


Scheme S-1: Synthesis of PAA-C≡CH.

- Estimation of the grafting degree of PEI-C≡CH by ^1H NMR.

We arbitrarily fixed the integration value of the signals resonating between 1.66 ppm and 0.97 ppm at 12 (according to the corresponding number of protons contained in the repetition unit of the polymer). From a comparison of the integration values of signals between 3.1 and 2.3 ppm (NCH₂CH₂N of the grafted 10-undecynoic acid), the effective degree of modification was estimated to be 12 %.

^1H NMR assignment in ppm (500 MHz, 10% D₂O): 3.35 (bs, NH₂CH₂), 3.18 (s, CONHCH₂CH₂), 2.92/2.76/2.63/2.55 (b, NCH₂CH₂N), 2.07 (bs, NHCOCH₂CH₂), 1.41/1.28/1.18 (b, CH₂CH₂CH₂).



Scheme S-2: Synthesis of PEI-C≡CH.

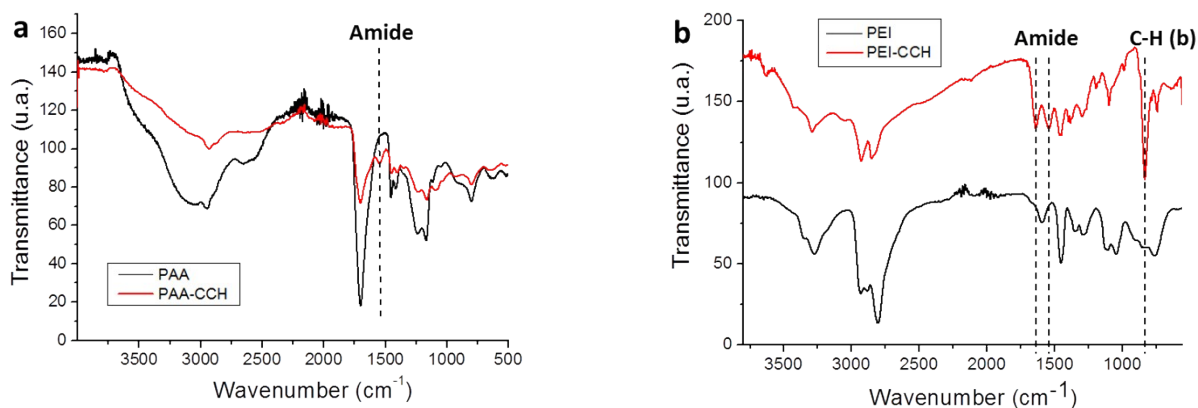


Figure S-2: ATR-FTIR Spectroscopy of functionalized polymers. a) ATR-FTIR spectra of PAA (black line) and PAA-C≡CH (red line). b) Typical ATR-FTIR spectra of PEI (black line) and PEI-C≡CH (red line) with characteristic bands of Amide 1540cm^{-1} and 1640cm^{-1} , and characteristic peak of the bending vibration C-H from the undecynoic acid grafted pendant chain.

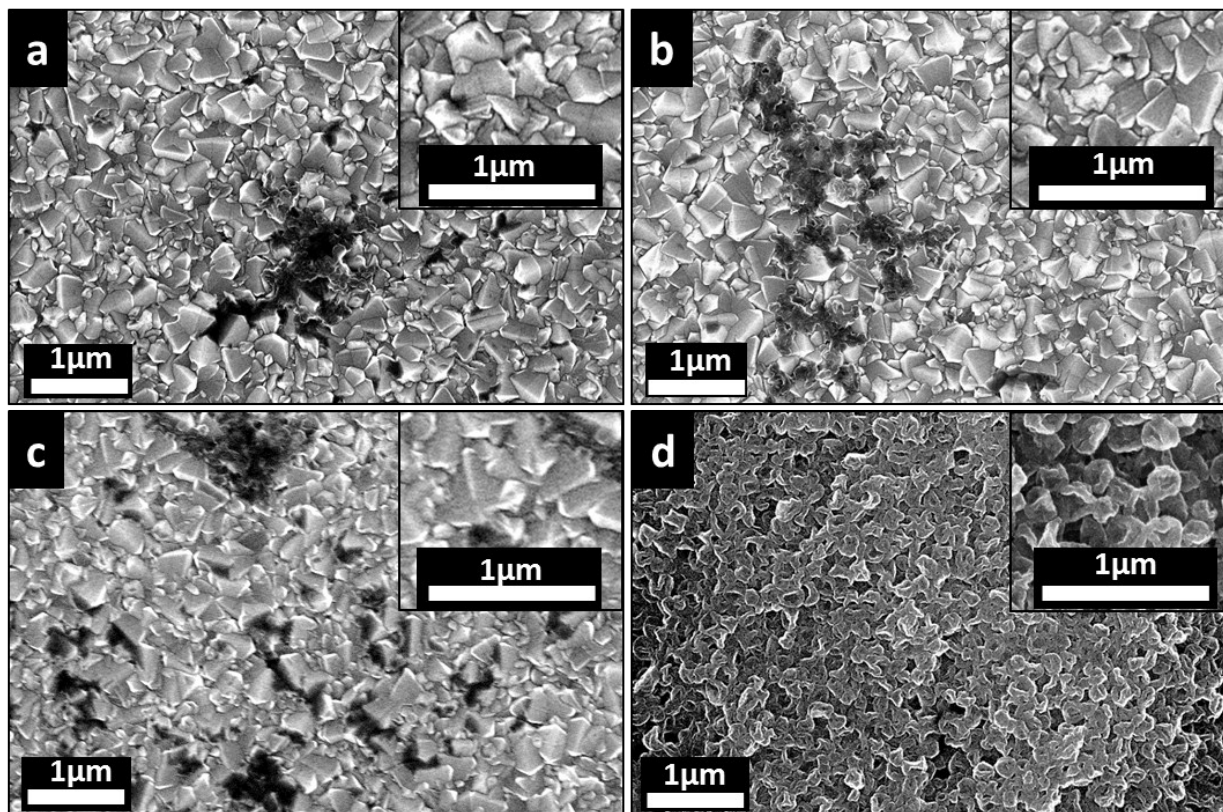
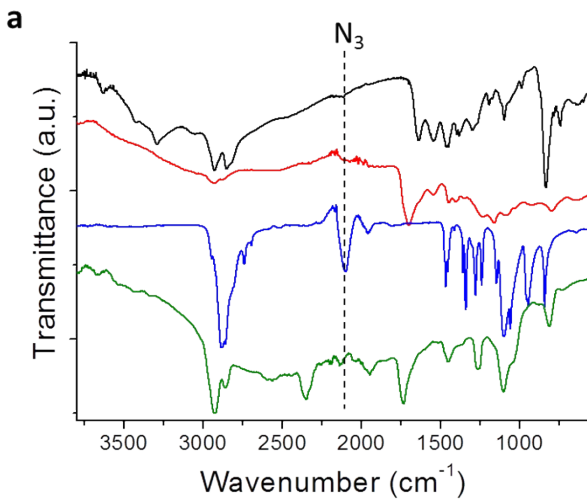


Figure S-3: Buildup of the film. Typical SEM micrographs of the deposited material on FTO (a) in absence of CuSO_4 , (b) in absence of $\text{N}_3\text{-PEG-N}_3$ linker, and (c) in absence of any applied potential. (d) Electro-clicked nanocapsule film obtained by using typical conditions (-0.2 V to 0.6 V vs Ag/AgCl , 50 mV/s in the presence of 4.5×10^9 Hybridosomes/mL 0.1 mg/mL $\text{N}_3\text{-PEG-N}_3$ and 0.6 mM CuSO_4 at $\text{pH } 3.5$).



b

Peak (cm^{-1})	Assignment	PEI-CC	PAA-CC	N_3 -PEG- N_3	Film
3630 - 3300	N-H (s)	■			■
2930 - 2850	N-H (s) O-H (s) C-H (s)	■	■	■	■
2340	CO_2 (s)				■
2100	N_3 (s)			■	
1954	C-H (b)			■	■
1730	C=O (s)		■		■
1638	N-H (b)	■			
1543	Amide (b)	■	■		
1455	C-H (sc)	■	■	■	■
1400	C-H (b)	■	■	■	■
1350	O-H (b)				
1335					
1297	C-H (b)	■		■	
1280	C-O (s)		■	■	■
1236	C-O-C (s)			■	
1190	C-N (s)	■			
1160		■	■		■
1146	C-O-C (s)			■	
1100	C-O (s) C-N (s)	■	■	■	■
1060	C-O-C (s)			■	■
1030	C-O (s)		■		
986 - 950	C-H (b)	■		■	
830 - 750	C-H ₂ (b) N-H (b)	■	■	■	■

Figure S-4: Click reaction occurrence. (a) ATR-FTIR spectra of PEI-C≡CH (black line), PAA-C≡CH (red line), N_3 -PEG- N_3 linker (blue line) and of the film (green line) constructed under typical conditions (-0.2 V to 0.6 V vs Ag/AgCl, 50 mV/s in the presence of 4.5×10^9 Hybridosomes/mL, 0.1 mg/mL N_3 -PEG- N_3 and 0.6 mM CuSO_4 at pH 3.5). (b) Corresponding peak assignments.

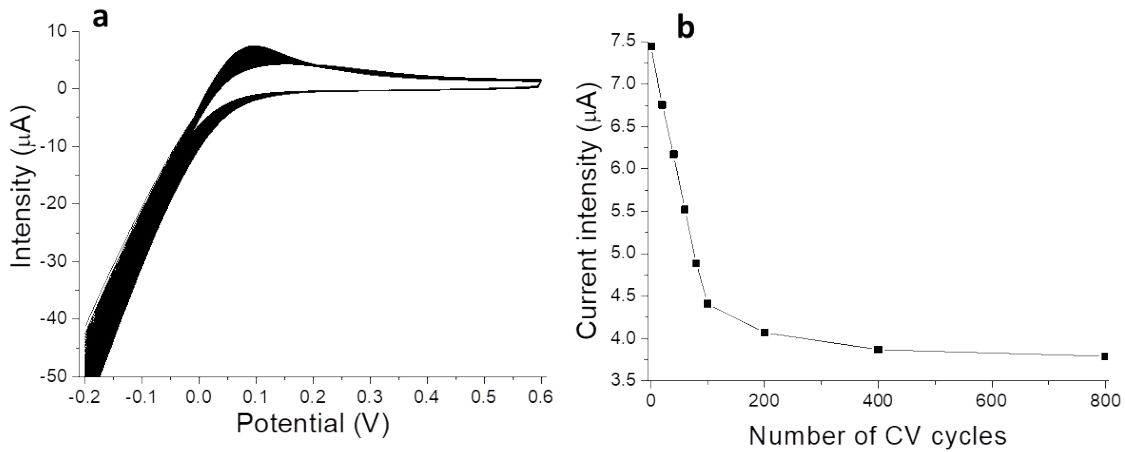


Figure S-5: Evolution of the intensity-potential diagram during the film construction. (a) Voltamogram corresponding to the buildup of a Hybridosome electrocycled film during 800 CV cycles under typical conditions (-0.2 V to 0.6 V vs Ag/AgCl, 50 mV/s in the presence of 4.5×10^9 Hybridosomes/mL, 0.1 mg/mL N_3 -PEG- N_3 and 0.6 mM $CuSO_4$ at pH 3.5). (b) Evolution of the maximum intensity of the copper oxidation peak, measured at 90 mV, in function of the CV cycle number.

CV number	Average surface coverage by the film (%)	Average thickness of the covered area (nm)	Roughness (RMS) of covered areas (nm)
0	0	0	33
25	11	138	80
100	75	541	78
800	92	845	122

Table S-1: Evolution of the film roughnesses during the electrocyclic deposition process. Roughnesses were obtained by calculating the root mean square (RMS) of the AFM cross-section data, in contact mode and in the dried state, corresponding to the area covered by the film, at 25, 100 and 800 CV cycles. The initial roughness of the FTO electrode (0 cycles) was calculated by calculating the RMS of the full AFM height image ($20 \times 20 \mu m^2$) of bare FTO.

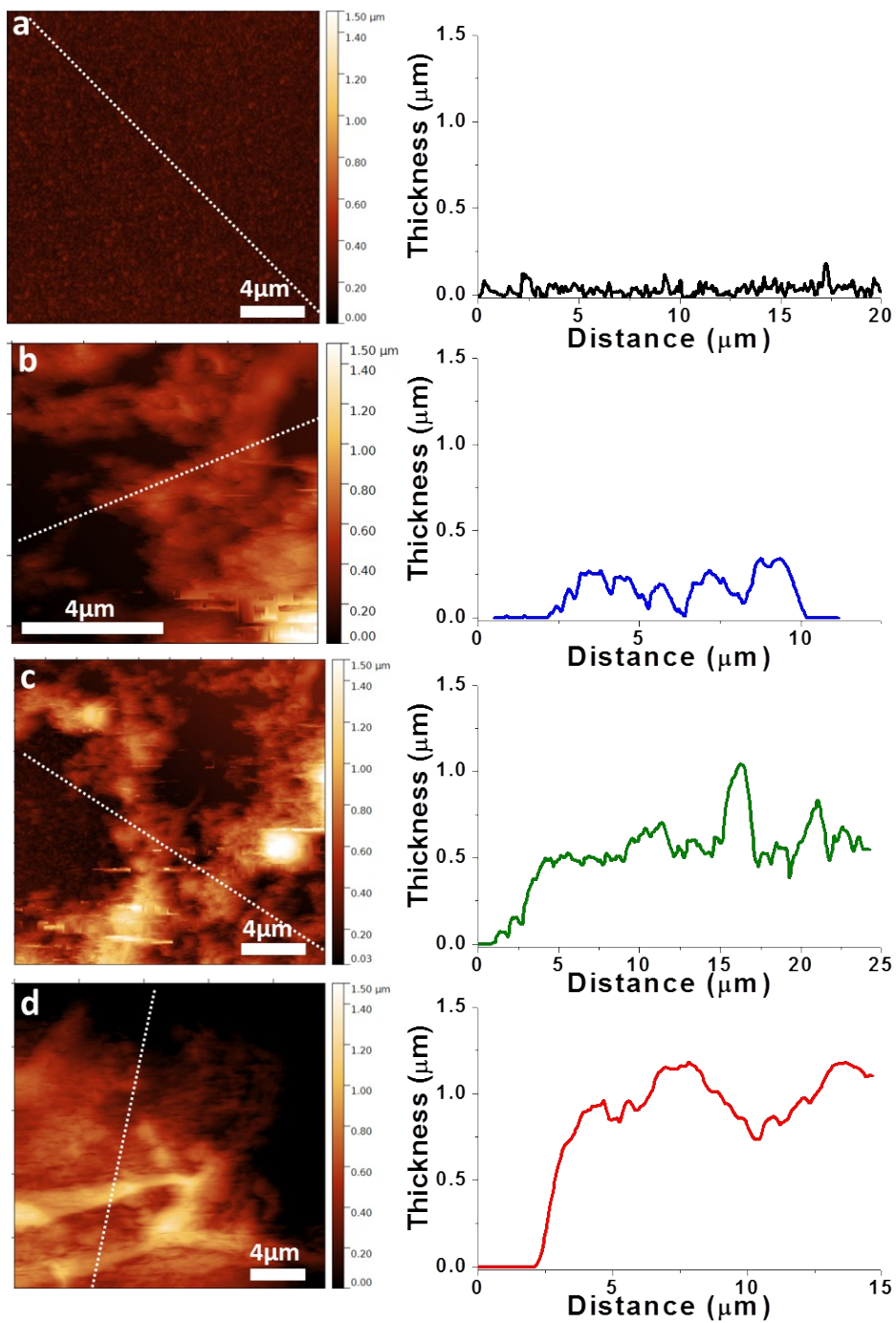


Figure S-6: Film growth, thickness evolution. AFM images and corresponding thickness profiles of (a) adsorbed Hybridosomes and films obtained under typical conditions after (b) 25, (c) 100 and (d) 800 CV cycles.

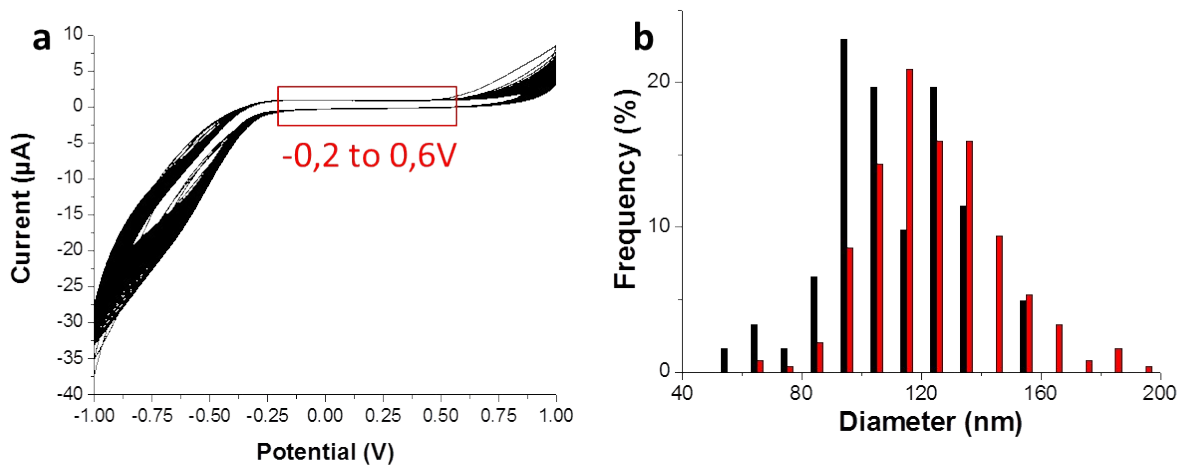


Figure S-7: Chemical and structural stability of Hybridosomes® along the film construction process. a) Voltamogram of 50 cycles from -1V to 1V (vs Ag/AgCl) at pH 3.5 of a Hybridosome dispersion. (b) Size distribution of Hybridosomes, calculated from low-magnification SEM micrographs with ImageJ, of adsorbed nanocapsules on a STEM grid (black bars) and after inclusion of the nanocapsules in the electro-clicked film (red bars).

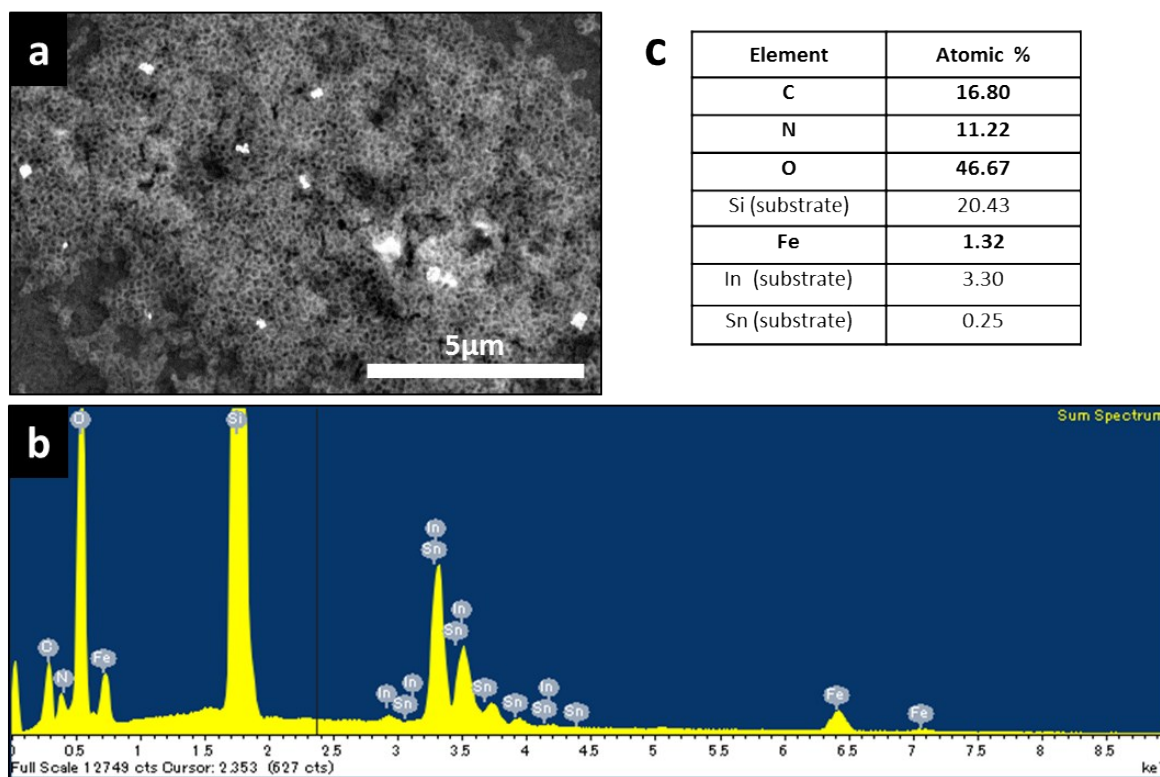


Figure S-8: Chemical composition of films constructed with IONPs based Hybridosomes®. a) SEM micrograph of a film assembled in typical electro-click conditions after 800 CV cycles. (b) Corresponding EDX analysis of the film. (c) Element analysis of the corresponding zone of the film.

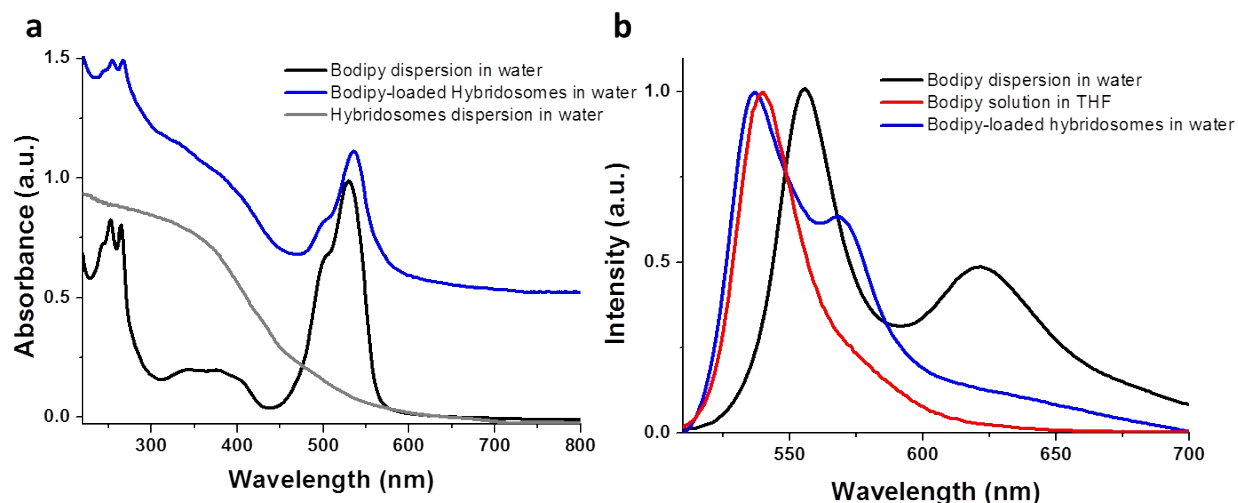


Figure S-9: BODIPY encapsulation, UV/Vis and Fluorescence spectra. a) UV/Vis absorbance spectra of aqueous dispersions of bodipy (black line), bodipy-loaded Hybridosomes (blue line) and « empty » Hybridosomes (grey line). (b) Fluorescence spectra (λ_{EX} at 480 nm) of bodipy dissolved in THF (red line), and aqueous dispersions of bodipy (black line) and bodipy-loaded Hybridosomes (blue line).

Loading efficiency of hybridosomes

The BODIPY dye absorbs both in solution and in the solid state. It is mostly water insoluble, so that we expect the BODIPY to be under the form of nanoprecipitated particles, both in the supernatant and in the core of the hybridosomes. Fig S-10a shows the absorbance spectra of the BODIPY-containing hybridosomes after washing twice (blue line), together with the supernatants of the first (black line) and second washes (red line). Importantly, the second supernatant is completely clear of bodipy, indicating that the encapsulated dye does not leak spontaneously. Note that the optical signal due to absorbance and scattering of the IONPs hybridosomes adds a significant background to the signal. However, after correction of the baselines, a rough comparison of the peaks area between the first wash supernatant and the bodipy-loaded hybridosomes, suggest that 73 % the bodipy was encapsulated.

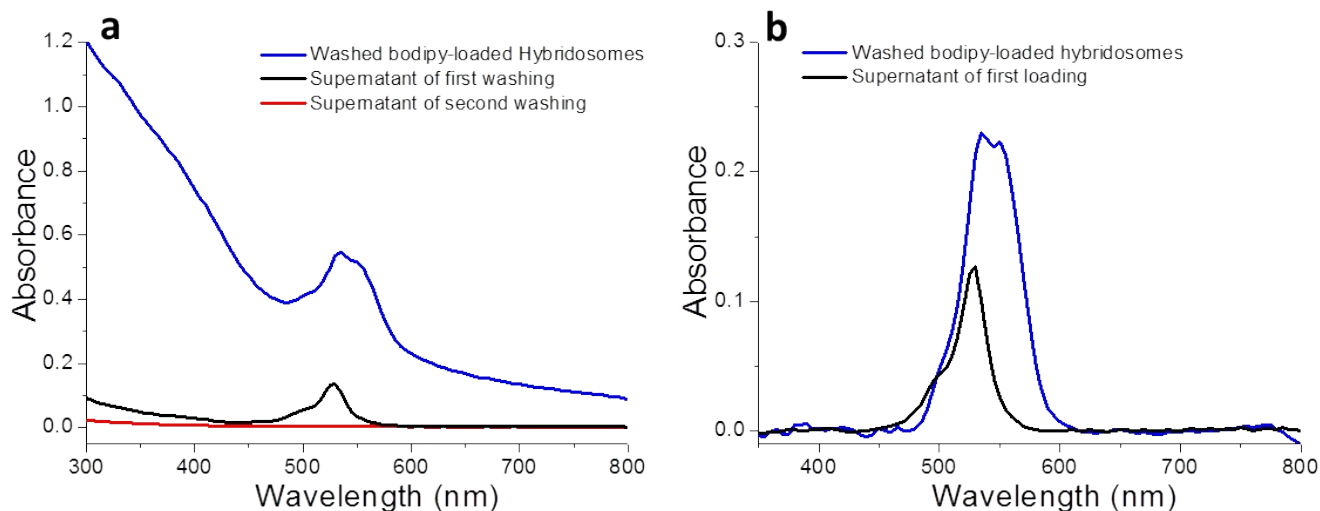


Figure S-10: Loading efficiency of hybridosomes. a) UV/Vis absorbance spectra of aqueous dispersions of bodipy (black line), bodipy-loaded Hybridosomes (blue line) and « empty » Hybridosomes (grey line). (b) Fluorescence spectra (λ_{EX} at 480 nm) of bodipy dissolved in THF (red line), and aqueous dispersions of bodipy (black line) and bodipy-loaded Hybridosomes (blue line).

L/E ratio (%)	Peak area (a.u.)
0	0
10	27 000
50	82 000
90	167 000

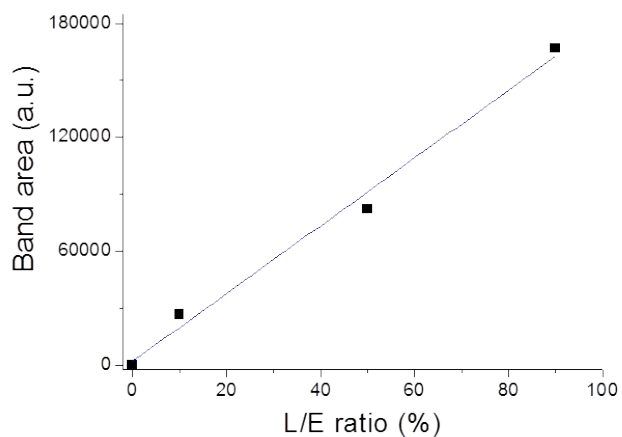


Figure S-11: Surface area of fluorescence emission bands (a) calculated by integration of the corresponding peaks between 510 nm and 700 nm. (b) Linear regression ($y = 1783.x + 2159$; $R^2=0.99$) of the peak areas in function of the “loading/empty” nanocapsules ratio in the building solution.

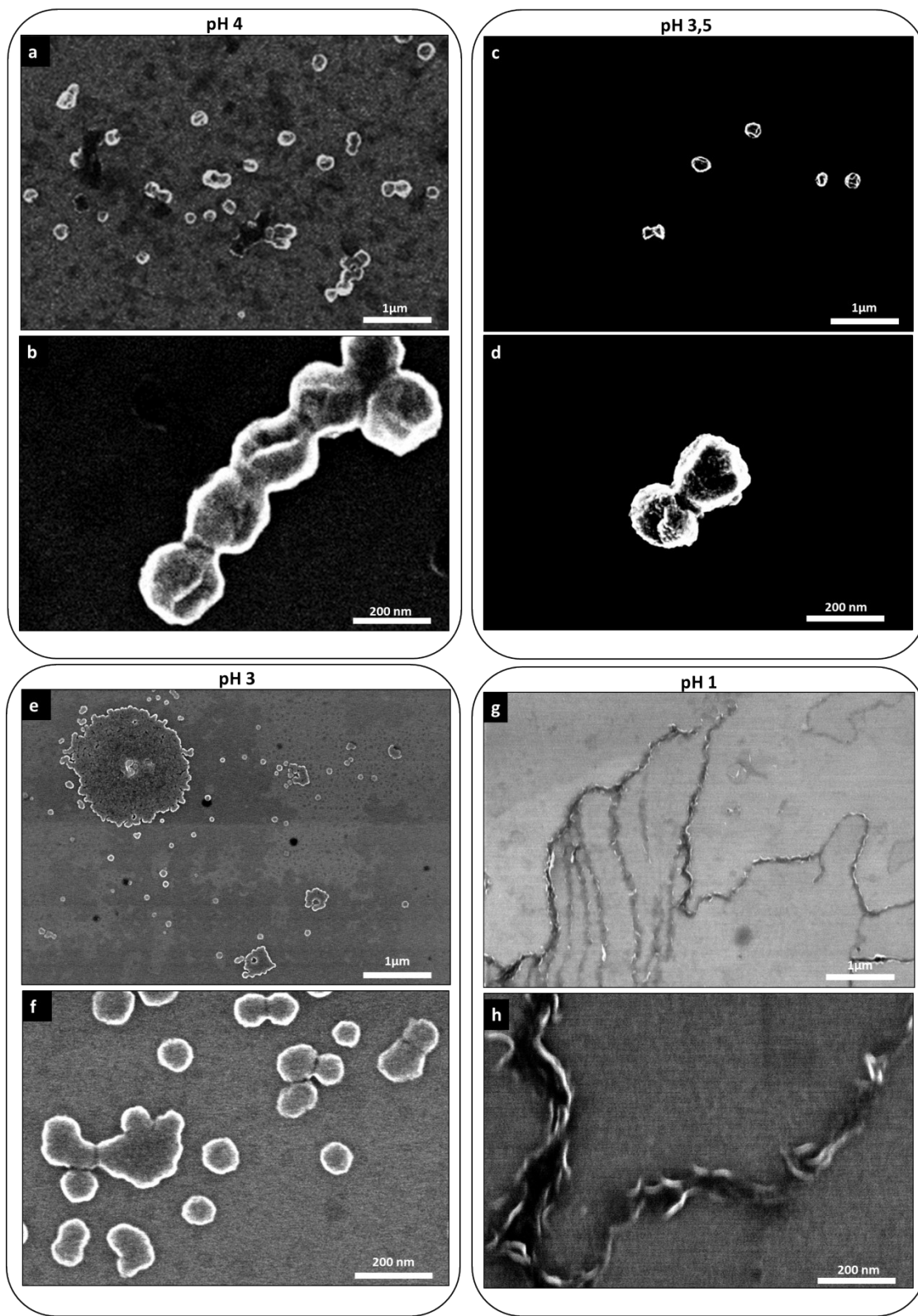


Figure S-12: pH sensitivity of functionalized “clickable” Hybridosomes® dispersions. Multiscale SEM analysis of Hybridosomes dispersions after 15 min of incubation with HCl solutions of pH 4 (a,b) pH 3.5 (c,d), pH 3 (e,f) and pH 1 (g,h).

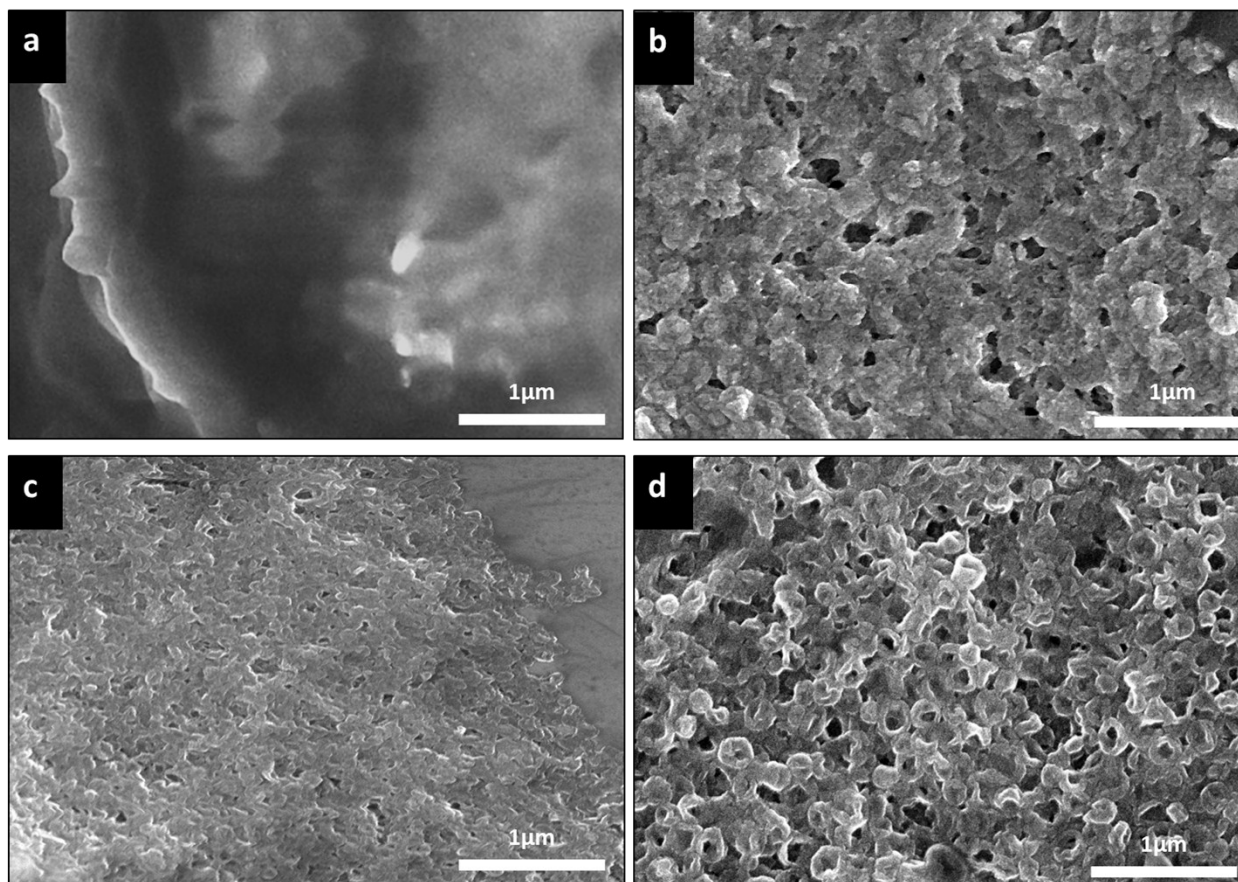


Figure S-13: pH sensitivity of electro-clicked Hybridosome®-based films. SEM micrographs of electro-clicked Hybridosome films obtained after 800 CV cycles and incubated 15 min in HCl solutions of pH 1 (a), pH 2.5 (b), pH 3 (c) and pH 3.5 (d).

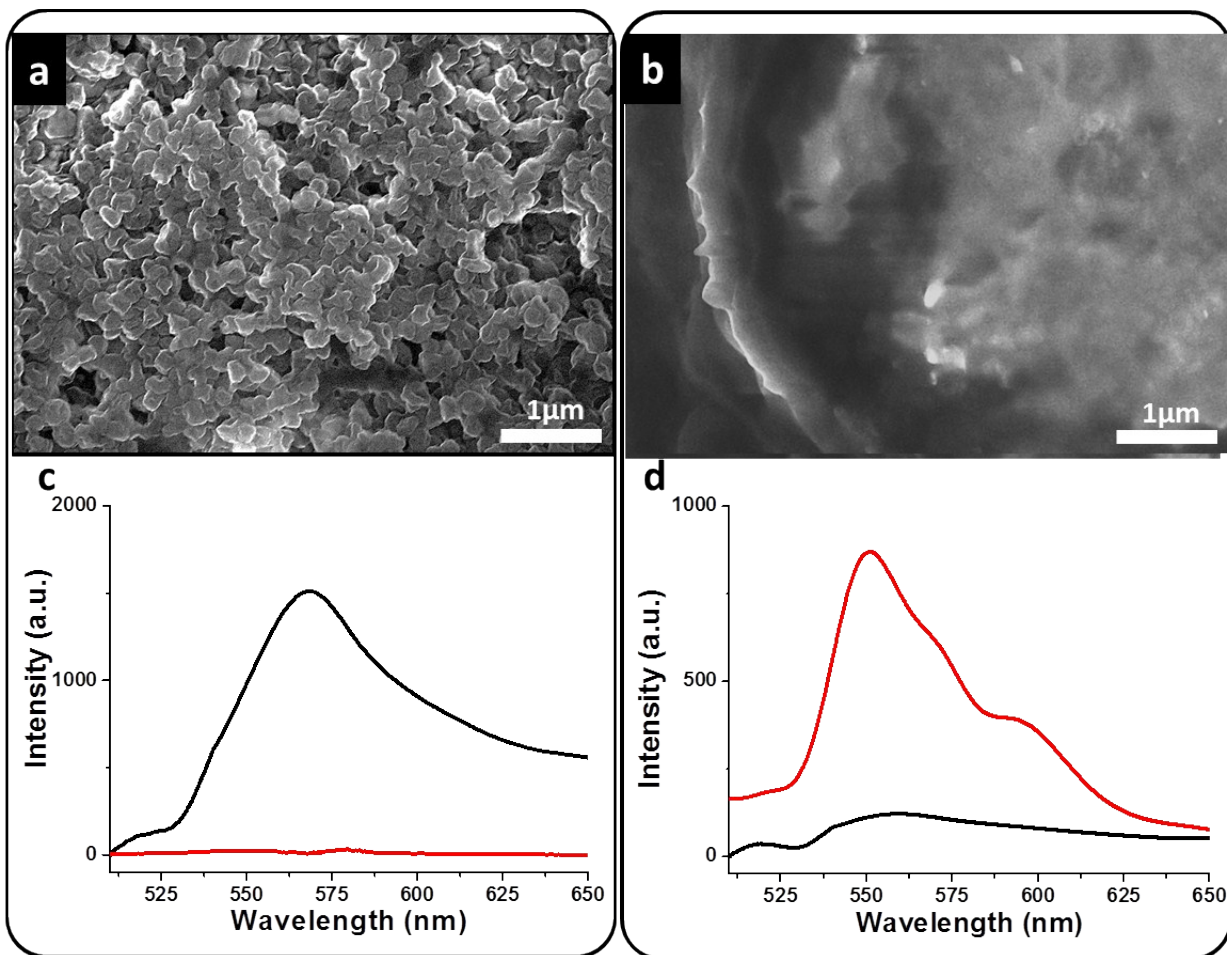


Figure S-14: pH-triggered release abilities of electro-clicked Hybridosomes®-based films. SEM micrographs (a, b) and fluorescence spectra (λ_{exc} at 480 nm) in the dry state (c, d) of bodipy-loaded Hybridosome films constructed on ITO (black line) and of the corresponding supernatant (red line) before (a,c) and after (b,d) application contact with a 0.1M HCl solution for 15min.

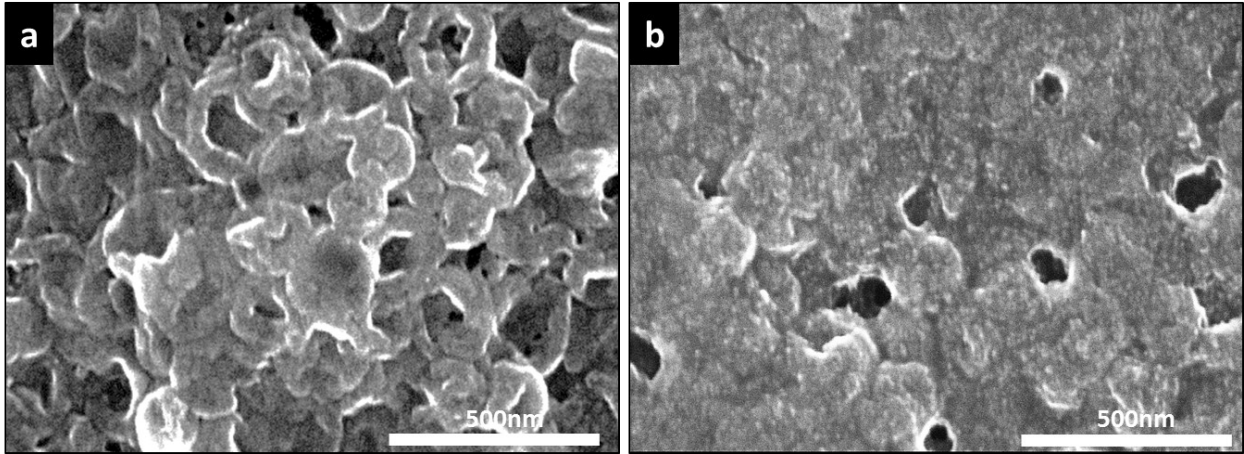


Figure S-15: Cargo release under electrochemical stimulus. SEM micrographs with higher magnification before (a) and after (b) applying +1 V potential vs Ag/AgCl for 15min in a 0.1M NaCl solution.